



Title	Structural and magnetic properties of epitaxially grown full-Heusler alloy Co <sub>2</sub> MnGe thin films deposited using magnetron sputtering
Author(s)	Ishikawa, Takayuki; Marukame, Takao; Matsuda, Ken-ichi et al.
Citation	Journal of applied physics, 99(8), 08J110-1-08J110-3 <a href="https://doi.org/10.1063/1.1270980">https://doi.org/10.1063/1.1270980</a>
Issue Date	2006-04-15
Doc URL	<a href="https://hdl.handle.net/2115/13461">https://hdl.handle.net/2115/13461</a>
Rights	(C) 2006 American Institute of Physics.
Type	journal article
File Information	JAP08J110_ishikawa.pdf



## Structural and magnetic properties of epitaxially grown full-Heusler alloy $\text{Co}_2\text{MnGe}$ thin films deposited using magnetron sputtering

Takayuki Ishikawa,<sup>a)</sup> Takao Marukame, Ken-ichi Matsuda, Tetsuya Uemura, Masashi Arita, and Masafumi Yamamoto

*Division of Electronics for Informatics, Graduate School of Information Science and Technology, Hokkaido University, Sapporo 060-0814, Japan*

(Presented on 3 November 2005; published online 25 April 2006)

Full-Heusler alloy  $\text{Co}_2\text{MnGe}$  thin films were epitaxially grown on  $\text{MgO}$  (001) substrates using magnetron sputtering. The films were deposited at room temperature and subsequently annealed *in situ* at temperatures ranging from 400 to 600 °C. X-ray pole figure measurements for the annealed films showed (111) peaks with fourfold symmetry, which gives direct evidence that these films are epitaxial and crystallized in the  $L2_1$  structure. Furthermore, cross-sectional transmission electron microscope images of a fabricated film indicated that it is single crystalline. The annealed films had sufficiently flat surface morphologies with roughnesses of about 0.26 nm rms at film thicknesses of 45 nm. The saturation magnetization of the annealed films was  $4.49 \mu_B/\text{f.u.}$  at 10 K, corresponding to about 90% of the Slater–Pauling value for  $\text{Co}_2\text{MnGe}$ . © 2006 American Institute of Physics. [DOI: 10.1063/1.2170980]

Half-metallic ferromagnets (HMFs)<sup>1</sup> are characterized by an energy gap for one spin direction at the Fermi level ( $E_F$ ), leading to a complete spin polarization at  $E_F$ . This feature of HMFs is highly favorable for ferromagnetic electrodes used in spintronic devices. Magnetic tunnel junctions (MTJs) using Co-based full-Heusler alloy thin films have recently been studied intensively<sup>2–5</sup> because of the half-metallic ferromagnetic nature theoretically predicted for some of these alloys<sup>6–8</sup> and because of their high Curie temperatures, which are well above room temperature (RT).<sup>9</sup> Using these thin films in MTJs requires abrupt, smooth interfaces. Hence, fully epitaxial MTJs are the most promising approach.  $\text{Co}_2\text{MnGe}$  (CMG) is one of the Co-based full-Heusler alloys that is theoretically predicted to be half-metallic.<sup>6,7</sup> Up to now, epitaxial  $L2_1$ -structured  $\text{Co}_2\text{MnGe}$  thin films have been grown on GaAs substrates using molecular beam epitaxy (MBE)<sup>10,11</sup> or pulsed laser deposition,<sup>12</sup> and spin injection from CMG into compound semiconductor heterostructures has been studied.<sup>11</sup> However, MTJs using a CMG thin film have not yet been developed. We recently reported a method of epitaxially growing Co-based full-Heusler alloy  $\text{Co}_2\text{Cr}_{0.6}\text{Fe}_{0.4}\text{Al}$  (CCFA) thin films on  $\text{MgO}$  substrates by magnetron sputtering and used it to fabricate fully epitaxial magnetic tunnel junctions with  $\text{MgO}$  tunnel barriers demonstrating relatively high tunnel magnetoresistance (TMR) ratios of 42% at RT and 74% at 55 K.<sup>5</sup> When we take into consideration that the lattice mismatch between CMG (lattice constant  $a=0.5743 \text{ nm}$ ) and  $\text{MgO}$  (diagonal length  $\sqrt{2} \times a_{\text{MgO}}=0.5957 \text{ nm}$ ) on a 45° in-plane rotation is relatively small ( $\approx -3.6\%$ ), comparable with that between CCFA and  $\text{MgO}$ , CMG is also a good candidate to be epitaxially grown on a  $\text{MgO}$  substrate by magnetron sputtering.

In this article, we report on the preparation of single-crystal CMG thin films epitaxially grown on  $\text{MgO}$  substrates

by magnetron sputtering and describe their structural and magnetic properties.

A 10-nm-thick  $\text{MgO}$  buffer layer was first grown on a  $\text{MgO}$  (001) single-crystal substrate at 400 °C to reduce or eliminate surface defects and microscopic roughness using electron beam evaporation at a deposition rate of 0.01 nm/s. Then the  $\text{Co}_2\text{MnGe}$  film was deposited on the  $\text{MgO}$  buffer layer using rf magnetron sputtering. These layers were successively deposited in an ultrahigh vacuum chamber (with a base pressure of around  $2 \times 10^{-7}$  Pa) incorporating magnetron sputtering with electron beam evaporation. The sputtering target used for preparing CMG thin films was an off-stoichiometric one. The CMG layers were deposited at a rate of 0.075 nm/s at RT and subsequently annealed *in situ* at 400–600 °C for 15 min. As a sputtering gas, Ar was used at a pressure of 0.1 Pa. The CMG film composition was analyzed using inductively coupled plasma optical emission spectroscopy for a 100-nm-thick CMG film deposited at RT. The CMG film composition was determined to be  $\text{Co}_{2.00}\text{Mn}_{1.05}\text{Ge}_{1.17}$  with an accuracy of 2%–3% for each element. Hereafter we represent the film composition as  $\text{Co}_2\text{MnGe}$  (CMG).

The structures of the fabricated CMG thin films were characterized using *in situ* reflection high-energy electron diffraction (RHEED), x-ray Bragg scans, x-ray pole figure measurements (Bruker AXS D8 DISCOVER Hybrid), electron diffraction, and cross-sectional high-resolution transmission electron microscope (HRTEM) observation. The surface morphologies were observed using atomic force microscopy (Digital Instruments). Magnetic properties were measured using a superconducting quantum interference device magnetometer (Quantum Design MPMS) at temperatures from RT to 10 K. For the estimation of magnetization ( $M$ ), the contribution from the  $\text{MgO}$  substrate was subtracted.

X-ray  $\theta-2\theta$  Bragg scans for as-deposited 45-nm-thick CMG films showed (004) peaks of CMG with low intensity, while clear (004) peaks with significantly higher intensity

<sup>a)</sup>Author to whom correspondence should be addressed; electronic mail: ishikawa@nsed.ist.hokudai.ac.jp

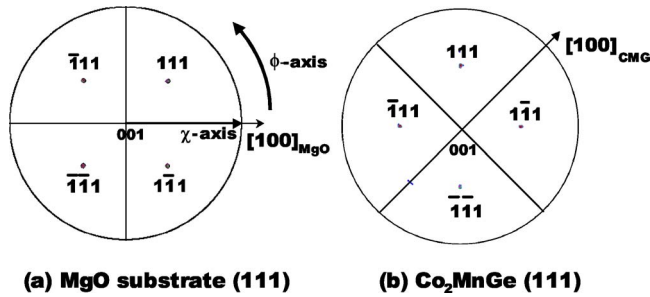


FIG. 1. X-ray pole figures of: (a) MgO substrate (111) and (b) Co<sub>2</sub>MnGe (111). The [100] direction of the Co<sub>2</sub>MnGe film is rotated by 45° from MgO [100] direction.

were observed for 400–600 °C-annealed films. In fact, the (004) peak of the 400 °C annealed film was about ten times more intense than that of the as-deposited film, and the (004) peak intensity further increased as the annealing temperature was increased from 400 to 600 °C. In the sense that the (004) peak intensity of CMG film was significantly increased by post-deposition annealing at 400–600 °C, the crystal structure of CMG film was improved by the annealing.

An x-ray pole figure scan of a CMG film deposited at RT and subsequently annealed at 600 °C is shown in Fig. 1, along with one of the MgO substrate. As can be seen in Fig. 1(a), MgO (111) diffraction peaks with fourfold symmetry with respect to the sample rotation angle,  $\phi$ , were observed at a tilt angle,  $\chi$ , of 54.7°. Here, we set the MgO [100] direction to the origin of the  $\phi$  axis. Figure 1(b) shows the fourfold symmetry of the CMG (111) peaks at  $\chi=54.7^\circ$ , which gives direct evidence that the 600 °C annealed film is epitaxial and crystallized in the  $L2_1$  structure. Because the  $\phi$  values for the CMG (111) peaks were shifted by 45° with respect to those of the MgO (111) peaks, the crystallographic relationship was CMG (001)[100]  $\parallel$  MgO (001)[110]. This relationship is reasonable in view of the relatively small lattice mismatch (–3.6%) between CMG (001) and MgO (001) on a 45° in-plane rotation. In contrast, in the x-ray pole figure scans for the as-deposited CMG thin films, (002) peaks were observed, while (111) peaks were not observed. These results indicate that the as-deposited CMG films were also grown epitaxially but with the  $B2$  structure. By annealing the as-deposited CMG film at temperatures ranging from 400 to 600 °C, the (111) peaks specific to the  $L2_1$  structure appeared and their intensity increased with increasing annealing temperature. Furthermore, microbeam electron dif-

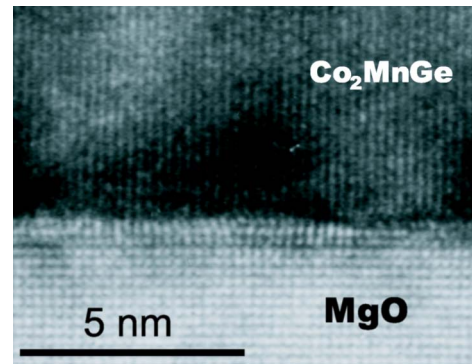


FIG. 2. Cross-sectional HRTEM lattice image, along  $[1\bar{1}0]$  direction of CMG, of heterostructure consisting of CMG layer (50 nm) and MgO buffer layer (10 nm). Vertical and horizontal directions correspond to CMG  $[001]$   $\parallel$  MgO  $[001]$  and CMG  $[110]$   $\parallel$  MgO  $[100]$  axis.

fraction patterns with beam diameters of 10–30 nm indicated that the fabricated film annealed at 600 °C had the  $L2_1$  structure with some residual regions of the  $B2$  and  $A2$  structures.

We also confirmed from the *in situ* RHEED observation along the two azimuths of  $[100]_{\text{MgO}}$  and  $[110]_{\text{MgO}}$  that the as-deposited CMG film on the MgO buffer layer had been grown epitaxially. The streak patterns of the CMG films annealed *in situ* at 600 °C were sharper and more distinct than those of the as-deposited film.

Figure 2 shows a cross-sectional HRTEM lattice image, along the  $[1\bar{1}0]$  direction of CMG, of a heterostructure consisting of a 50-nm-thick CMG film annealed at 600 °C and a 10-nm-thick MgO buffer layer. It clearly indicates that both the MgO buffer layer and the CMG layer were epitaxially grown and are single-crystalline. Furthermore, as is shown in Fig. 2, the interface between the CMG layer and MgO buffer layer was abrupt and highly smooth, although dislocations formed to relax the lattice mismatch of –3.6% between CMG and MgO were observed at some parts of the CMG/MgO interface.

Lower ferromagnetic electrodes with little surface roughness must be prepared to fabricate high-quality MTJs. Figure 3(a) shows a typical 3D surface image of a 45-nm-thick CMG film deposited on a 10-nm-thick MgO buffer layer at RT and subsequently annealed at 600 °C. As shown in the figure, the film had sufficiently flat surface morphologies with roughness of about 0.26 nm rms. The annealing temperature dependence of the surface roughness of the 45-nm-thick CMG film is shown in Fig. 3(b). The figure clearly shows that post-deposition annealing improved the surface roughness from that of 0.40 nm rms for as-deposited films, which is consistent with the *in situ* RHEED observations. For comparison, we also prepared as reference samples CMG films that were directly deposited at a substrate temperature of 400 °C and measured their surface roughness. The rms values of roughness of those films were about 0.72 nm or more. These results clearly indicated that the fabrication procedure of depositing films at RT and subsequently annealing *in situ* is advantageous for obtaining sufficiently flat surface morphologies in these films.

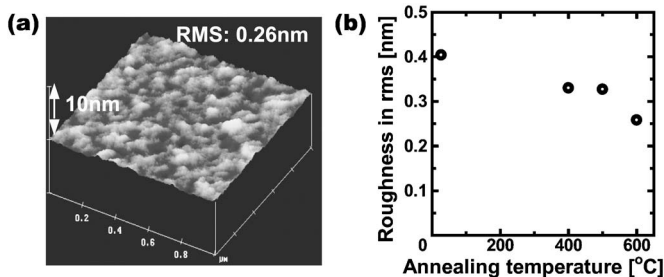


FIG. 3. (a) Three-dimensional AFM image of surface topography of 45-nm-thick Co<sub>2</sub>MnGe film annealed at 600 °C. (b) Annealing temperature dependence of surface roughness of 45-nm-thick Co<sub>2</sub>MnGe films.

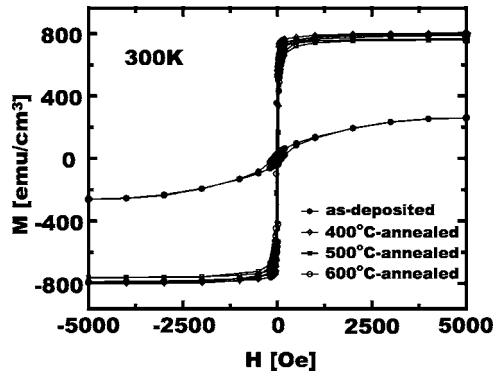


FIG. 4.  $M$ - $H$  curves up to 5000 Oe for 45-nm-thick  $\text{Co}_2\text{MnGe}$  thin films annealed at temperatures ranging from 400 to 600 °C in comparison with that for as-deposited film with magnetic field applied in film plane along  $[110]$  direction of  $\text{Co}_2\text{MnGe}$  at 300 K. Magnetization due to substrate has been subtracted.

Figure 4 shows the magnetization curves up to a magnetic field,  $H$ , of 5000 Oe for 45-nm-thick CMG thin films annealed at temperatures ranging from 400 to 600 °C. The saturation magnetization,  $\mu_s$ , was extracted from the hysteresis curves. The annealing temperature dependences of  $\mu_s$  and coercive force,  $H_c$ , for 45-nm-thick thin films at 300 and 10 K are shown in Fig. 5. For as-deposited films, the  $\mu_s$  observed at 10 K was  $1.71 \mu_B$  per formula unit (f.u.).

This  $\mu_s$  value was only about one-third that of bulk CMG ( $5.11 \mu_B/\text{f.u.}$ ) observed at a low temperature.<sup>9</sup> After post-deposition annealing at 400–600 °C, the  $\mu_s$  increased significantly (up to about 2.6 times the as-deposited value of  $1.71 \mu_B/\text{f.u.}$ ). The  $\mu_s$  value of  $4.49 \mu_B/\text{f.u.}$  at 10 K obtained for the 600 °C annealed film corresponds to about 90% of the theoretically predicted Slater–Pauling value of  $5.0 \mu_B/\text{f.u.}$  for CMG with the  $L2_1$  structure.<sup>8</sup> Furthermore, the  $H_c$  value of approximately 100 Oe at 300 K ( $\sim 300$  Oe at 10 K) for as-deposited films significantly decreased after post-deposition annealing, resulting in  $H_c$  values ranging from 3.9 Oe (400 °C annealed) to 29 Oe (600 °C annealed) at 300 K (ranging from 6.4 to 32 Oe at 10 K). The  $H_c$  value of 29 Oe observed at 300 K for the 600 °C annealed film is comparable with that of the CMG film (approximately 40 Oe at RT) grown using MBE on a GaAs substrate.<sup>10</sup> The pronounced improvement of the magnetic properties in terms of  $\mu_s$  and  $H_c$  using postdeposition annealing is probably related

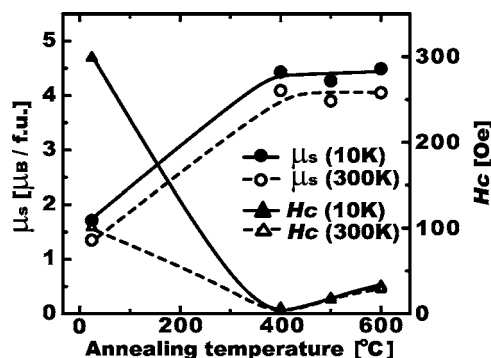


FIG. 5. Annealing temperature dependences of saturation magnetization,  $\mu_s$ , and coercive force,  $H_c$ , at 10 and 300 K for 45-nm-thick  $\text{Co}_2\text{MnGe}$  thin films. Magnetic field direction was same as that for Fig. 4.

to the crystal structure improvement in terms of the increased (004) peak intensity and the appearance of the  $L2_1$  structure using postdeposition annealing at 400–600 °C. Note that  $H_c$  increased slightly with increasing annealing temperature from 400 to 600 °C. To clarify the origin of the slight increase of  $H_c$  with increasing annealing temperature from 400 to 600 °C, further studies should be carried out.

Given the epitaxially grown, single-crystalline CMG films with excellent surface flatness, we fabricated MTJs with the following layer structure: MgO buffer layer (10 nm)/CMG lower electrode (50 nm)/MgO tunnel barrier (2.5–3.0 nm)/ $\text{Co}_{50}\text{Fe}_{50}$  (CoFe) upper electrode (10 nm), grown on an MgO (001) substrate. The MgO tunnel barrier was deposited by electron beam evaporation at RT. The cross-sectional HRTEM lattice image of a fabricated MTJ layer structure distinctively indicated that all layers, including the CMG lower electrode, the MgO tunnel barrier, and the CoFe upper electrode, were grown epitaxially and single crystalline. The microfabricated MTJs exhibited the strongly temperature-dependent TMR ratios of 14% at RT and 70% at 7 K. The spin-dependent magnetotransport properties of the fabricated MTJs will be reported separately.<sup>13</sup>

In summary, single-crystal full-Heusler alloy  $\text{Co}_2\text{MnGe}$  thin films were epitaxially grown on MgO (001) substrates using magnetron sputtering. The  $\text{Co}_2\text{MnGe}$  thin films were deposited at RT and subsequently annealed *in situ* at 400–600 °C. X-ray pole figure measurements showed that the annealed films were epitaxial and crystallized in the  $L2_1$  structure. The annealed films had sufficiently flat surface morphologies. The saturation magnetization of the annealed films was  $4.49 \mu_B/\text{f.u.}$  at 10 K, corresponding to about 90% of the Slater–Pauling value for  $\text{Co}_2\text{MnGe}$ . Given these epitaxial  $\text{Co}_2\text{MnGe}$  thin films, fully epitaxial magnetic tunnel junctions using a  $\text{Co}_2\text{MnGe}$  thin film and a MgO tunnel barrier were fabricated.

<sup>1</sup>R. A. Groot, F. M. Mueller, P. G. van Engen, and K. H. J. Buschow, *Phys. Rev. Lett.* **50**, 2024 (1985).

<sup>2</sup>K. Inomata, S. Okamura, R. Goto, and N. Tezuka, *Jpn. J. Appl. Phys., Part 2* **42**, L419 (2003).

<sup>3</sup>S. Kämmerer, A. Thomas, A. Hütten, and G. Reiss, *Appl. Phys. Lett.* **85**, 79 (2004).

<sup>4</sup>H. Kubota, J. Nakata, M. Oogane, Y. Ando, A. Sakuma, and T. Miyazaki, *Jpn. J. Appl. Phys., Part 2* **43**, L984 (2004).

<sup>5</sup>T. Marukame, T. Kasahara, K.-i. Matsuda, T. Uemura, and M. Yamamoto, *Jpn. J. Appl. Phys., Part 2* **44**, L521 (2005); T. Marukame, T. Kasahara, K.-i. Matsuda, T. Uemura, and M. Yamamoto, *IEEE Trans. Magn.* **41**, 2603 (2005).

<sup>6</sup>S. Ishida, S. Fujii, S. Kashiwagi, and S. Asano, *J. Phys. Soc. Jpn.* **64**, 2152 (1995).

<sup>7</sup>S. Picozzi, A. Continenza, and A. J. Freeman, *Phys. Rev. B* **66**, 094421 (2002).

<sup>8</sup>I. Galanakis, P. H. Dederichs, and N. Papanikolaou, *Phys. Rev. B* **66**, 174429 (2002).

<sup>9</sup>P. J. Webster, *J. Phys. Chem. Solids* **32**, 1221 (1971).

<sup>10</sup>T. Ambrose, J. J. Krebs, and G. A. Print, *J. Appl. Phys.* **87**, 5463 (2000).

<sup>11</sup>X. Y. Dong, C. Adelman, J. Q. Xie, C. J. Palmstrom, X. Lou, J. Strand, P. A. Crowell, J.-P. Barnes, and A. K. Petford-Long, *Appl. Phys. Lett.* **86**, 102107 (2005).

<sup>12</sup>B. Ravel, J. O. Cross, M. P. Raphael, V. G. Harris, R. Ramesh, and V. Saraf, *Appl. Phys. Lett.* **81**, 2812 (2002).

<sup>13</sup>T. Marukame, T. Ishikawa, K.-i. Matsuda, T. Uemura, and M. Yamamoto, Paper No. 050646AC09, *J. Appl. Phys.* (these proceedings).